

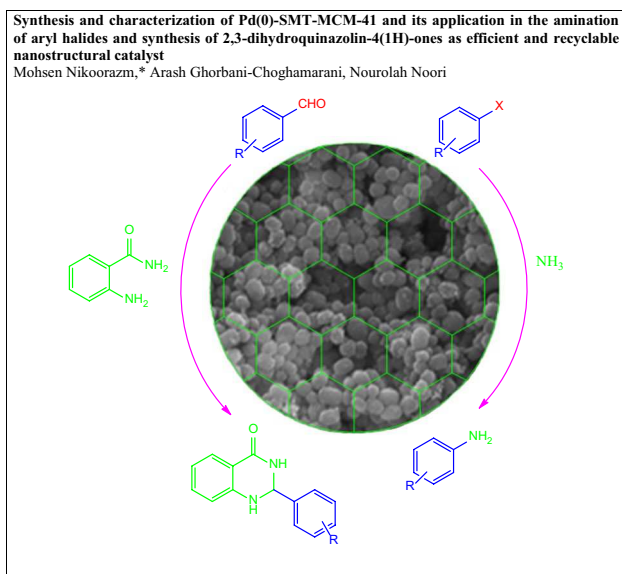
Synthesis and Characterization of Pd(0)-SMT-MCM-41 and its Application in the Amination of Aryl Halides and Synthesis of 2,3-Dihydroquinazolin-4(1H)-Ones as Efficient and Recyclable Nanostructural Catalyst

Nourolah Noori¹ · Mohsen Nikoorazm¹ · Arash Ghorbani-Choghamarani¹

Received: 31 July 2016 / Accepted: 30 October 2016
© Springer Science+Business Media New York 2016

Abstract Palladium S-methylisothiurea [Pd(0)-SMT] has been grafted at the surface of functionalized mesoporous silica MCM-41 and used as an efficient and reusable heterogeneous nanocatalyst system for amination of various aryl halides and the one-pot synthesis of 2,3-dihydroquinazolin-4(1H)-one derivatives. The present methodology offers several advantages such as simplicity of procedure, easy isolation of the products and reused for several consecutive runs without significant loss of their catalytic efficiency. The characteristic structural features of this new catalyst was determined by various physico-chemical techniques such as FT-IR spectroscopy, XRD, SEM/EDS, ICP, TGA, BET surface area measurement and elemental analysis.

Graphical Abstract



Keywords Pd(0)-SMT-MCM-41 · Reusable nanocatalyst · Amination of aryl halides · 2,3-Dihydroquinazolin-4(1H)-one

1 Introduction

Considerable research efforts have been made in the recent years towards development of silica mesoporous nanocomposite in particular MCM-41 as immobilized support [1, 2]. This silica mesoporous has hexagonal arrangement of one dimensional mesoporous with large pore size in the range 20–100 Å. Due to its exclusive properties such as high surface area, high pore volume (1.3 cm³ g⁻¹), great diversity

✉ Mohsen Nikoorazm
e_nikoorazm@yahoo.com

¹ Department of Chemistry, Faculty of Science, Ilam University, P.O. Box 69315516, Ilam, Iran

in surface functionalization, homogeneity of the pores, good thermal stability, accessible and tunable pores and has attracted extensive attention [3–6]. MCM-41 has the potential to be applied as catalyst support, adsorption [7] environmental purification [8], drug delivery [9] and host for the inclusion of bulkier guest molecules such as enzymes and organometallic compounds [10]. The appearance of the chemistry of transition metals in the 1960s has deeply changed the science of organic synthesis [11]. Palladium metal is classified as a transition metal which provides excellent opportunities for catalytic reactions. Generally, the activity of homogeneous palladium catalysts is sufficiently high; however, these catalysts show as a major drawback a difficult recycling and separation from the product which have limited their applications [12, 13]. In order to overcome the above drawbacks, heterogenisation of palladium complexes via immobilization/grafting onto solid supports especially MCM-41 has attracted great attention because of its typical properties of easy separation, catalyst recycling; it is also a great catalyst for transformation reactions and in industrial fine chemical synthesis [14–17]. Aniline is an important organic chemical for constructing natural products and is widely used as intermediates for the production of medicine, dye, resin etc [18–20]. Therefore, the development of highly efficient procedure for the single step production of aniline via direct amination of aryl halides under mild reaction conditions has acquire important attention in green chemistry and synthetic chemistry [10, 21]. On the other hand, 2,3-dihydro-4(1H)-quinazolinones derivatives are an important class of heterocyclic compounds which have appeared as versatile biologically active compounds possessing applications as vasodilating, tranquilizing, diuretic, antibiotic, antitumor, anticancer, herbicidal activity, antihypertensive agents and plant growth regulation ability [22–24]. Generally, 2,3-dihydroquinazolin-4(1H)-ones were synthesized using the reductive cyclization of ketones or aldehydes with 2-aminobenzamide in the presence of acid catalysts [25]. Thus, there is a necessity to develop a simple and efficient method for the synthesis of 2, 3-dihydroquinazolin-4(1H)-ones derivatives in high yields under mild reaction conditions. The present work describes synthesis and characterization of Pd complex immobilized onto MCM-41 [Pd(0)-SMT-MCM-41] which is used as a novel and efficient catalyst for the synthesis of 2, 3-dihydroquinazolin-4(1H)-ones derivatives through the reaction of aromatic aldehydes and anthranilamide and anilines from amination of aryl halides.

2 Experimental

2.1 Materials

The tetraethylorthosilicate (TEOS), cationic surfactant cetyltrimethylammonium bromide (CTAB, 98%),

3-chloropropyltrimethoxy silane (3-CIPTES), sodium hydroxide, s-methyl isothiourrea, palladium acetate and solvents were purchased from Merck, Aldrich or Flucka companies.

2.2 Measurements

IR analyses were carried out on FTIR as KBr pellets, spectrophotometer (Bruker, Germany) Vertex 70 in the range of 400–4000 cm^{-1} . The physico-chemical characteristics were carried out using X-ray powder diffraction (XRPD) on a Philips diffractometer of X'pert company with monochromatized Cu K α radiation under the conditions of 40 kV, $\lambda = 1.5418 \text{ \AA}$ and 30 mA. N_2 adsorption–desorption isotherm and BJH pore size were recorded by (BELSORP-MINI), TGA of the samples was carried out using a Shimadzu DTG-60 automatic thermal analyzer in the temperature range 30–900 °C at a heating rate of 10 °C min^{-1} in air. The transmission electron micrographs (TEM) were obtained with a Philips CM10 microscope, working at 200 kV accelerating voltage. The particle morphology was recorded by measuring SEM using FESEM-TESCAN MIRA3. The content of Pd was measured using inductively coupled plasma-optical emission spectrometry (ICP-OES, perkin elmer, optima 800) and elemental analysis was carried out on COSTECH, England CHNS elemental analysis.

2.3 Synthesis of (3-Chloropropyl) Trimethoxysilane Functionalized MCM-41

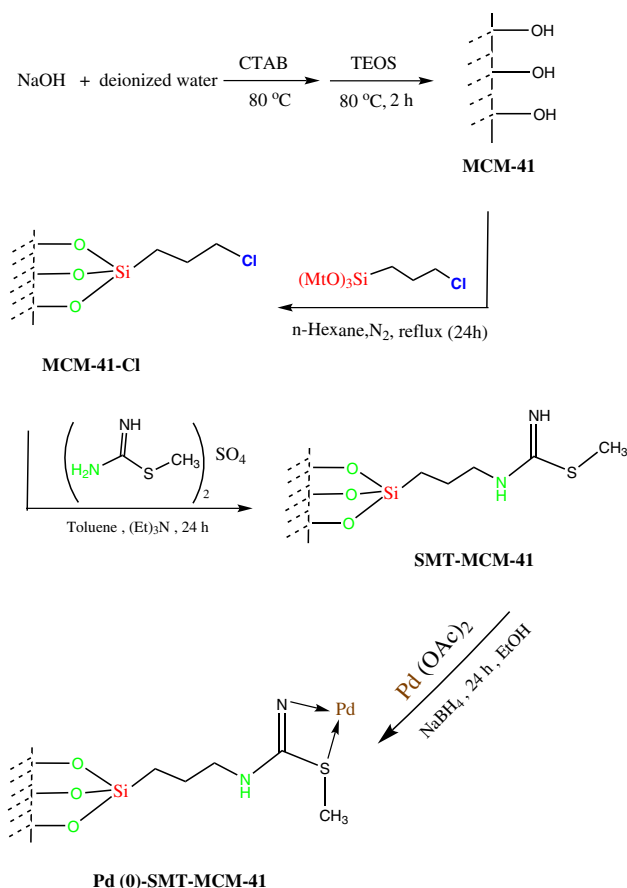
The synthesis of nanosized MCM-41 was carried out by the sol–gel method using tetraethylorthosilicate (TEOS) as the Si source, cetyltrimethylammonium bromide (CTAB) as the template, and sodium hydroxide as the pH control agent. In a typical procedure, to the solution of NaOH (2 M, 3.5 mL) in deionized water (480 mL) at 80 °C, surfactant CTAB (2.74 mmol, 1 g) was added. After the solution became homogeneous, TEOS (5 mL) was added dropwise to the solution under continuous stirring at 80 °C, and the mixture was stirred under reflux for 2 h. The mixture was cooled to the room temperature and the resulting solid was gathered by filtration, washed with deionized water and dried in an oven at 60 °C and followed by calcination at 550 °C for 5 h with rate of 2 °C min^{-1} . Finally, we obtained the mesoporous MCM-41. Then Mesoporous silica (MCM-41) (1 g) was added to a solution of 3-chloropropyltrimethoxy silane (1 g) in n-Hexane (100 mL) and refluxed for 24 h. The resulting white solid MCM-41-($\text{SiCH}_2\text{CH}_2\text{CH}_2\text{Cl}$) $_x$ was filtered, and washed repeatedly with n-hexane and finally dried under vacuum.

2.4 Synthesis of s-Methyl Isothiourea on Functionalized MCM-41

To the mixture of functionalized MCM-41 (1 g) and s-methyl isothiourea (0.138 g) in toluene (30 mL), triethylamine (1.5 mmol) were added and stirred under reflux conditions for 24 h. After completion of the reaction, the resulting solid was filtered, washed with ethanol and finally dried to obtain SMT-MCM-41 (Scheme 1).

2.5 Synthesis of the Pd(0)-SMT-MCM-41 Heterogeneous Catalyst

Pd(0)-SMT-MCM-41 was synthesized by stirring a mixture of SMT-MCM-41 (1 g), palladium acetate (0.5 g) in ethanol (50 mL) for 20 h under reflux conditions. Then, sodium borohydride (0.6 g) was added to this mixture and kept under reflux for 4 h. Finally, the resulting catalyst was filtered, washed several times with ethanol, dried at 50 °C for 24 h (Scheme 1).



Scheme 1 Synthesis of Pd(0)-SMT-MCM-41 heterogeneous catalyst

2.6 General Procedure for Synthesis of Amination of Aryl Halides

In a typical procedure, a mixture of aryl halide (1 mmol) and ammonium hydroxide (28%) (1 mL, 0.003 mmol), 0.010 g of Pd(0)-SMT-MCM-41 as catalyst was added and the reaction mixture was stirred at room temperature for an appropriate time (Table 3). The progress of the reaction is followed by TLC. After completion of the reaction, the product was extracted with ethyl acetate (3 × 10 mL). The combined extracts were dried with Na₂SO₄ followed by the evaporation of the solvent, yielding the corresponding product with excellent yield.

2.7 General Procedure for the Synthesis of 2,3-Dihydroquinazolin-4(1H)-Ones Derivatives

A reaction tube was charged with anthranilamide (1 mmol), aldehyde (1 mmol) and Pd(0)-SMT-MCM-41 (0.01 g) was stirred at 80 °C in ethanol (2 mL) for the appropriate time (Table 5). The progress was monitored by TLC. Upon completion, the reaction mixture was cooled to room temperature, then, catalyst was separated by simple filtration and the product was extracted with CH₂Cl₂ (2 × 5 mL). Finally by the evaporation of the solvent from the filtrate, the desired products were obtained.

2.8 Selected Spectral Data

2.8.1 Aniline (Entry 1 and 2, Table 3)

¹H NMR (400 MHz, CDCl₃): δ_H = 7.26–7.24 (m, 2H), 6.87–6.83 (tt, *J* = 7.2 Hz, 1H), 6.77–6.73 (m, 2H), 3.66 (s, 2H) ppm.

2.8.2 4-Chloroaniline (Entry 3, Table 3)

¹H NMR (400 MHz, CDCl₃): δ_H = 7.14–7.11 (dt, *J* = 8.8 Hz, 2H), 6.65–6.61 (dt, *J* = 8.8 Hz, 2H), 3.58 (broad, 2H) ppm.

2.8.3 4-Nitroaniline (Entry 7, Table 3)

¹H NMR (400 MHz, CDCl₃): δ_H = 8.11–8.08 (d, *J* = 9.2 Hz, 2H), 6.66–6.64 (d, *J* = 8.8 Hz, 2H), 4.42 (broad, 2H) ppm.

2.8.4 Pyridin-2-Amine (Entry 8, Table 3)

¹H NMR (400 MHz, CDCl₃): δ_H = 8.06–8.04 (d of t, *J* = 5.2 Hz, 1H), 7.42–7.37 (td, *J* = 7.6 Hz, 1H), 6.65–6.62

(t of d, $J = 6$ Hz, 1H), 6.51–6.49 (d, $J = 8.8$ Hz, 1H), 4.65 (s, 2H) ppm.

2.8.5 2-(4-Chlorophenyl)-2,3-Dihydroquinazolin-4(1H)-One (Entry 6, Table 5)

^1H NMR (400 MHz, DMSO- d_6): $\delta_{\text{H}} = 8.29$ (s, 1H), 7.62–7.42 (m, 5H), 7.25–7.21 (t, $J = 7.5$, 1H), 7.11 (s, 1H), 6.74–6.62 (m, 2H), 5.74 (s, 1H) ppm.

2.8.6 2-(4-Ethoxyphenyl)-2,3-Dihydroquinazolin-4(1H)-One (Entry 4, Table 5)

^1H NMR (400 MHz, DMSO- d_6): $\delta_{\text{H}} = 7.94$ –7.93 (b, 1H), 7.53–7.51 (m, 2H), 7.33 (s, 1H), 7.25 (s, 1H), 6.94–6.91 (m, 3H), 6.67–6.68 (m, 1H), 5.84 (s, 1H), 5.74 (s, 1H), 4.04–4.06 (q, $J = 4$, 2H), 1.45–1.43 (s, 3H) ppm.

2.8.7 2-(4-Methylphenyl)-2,3-Dihydroquinazolin-4(1H)-One (Entry 2, Table 5)

$\delta_{\text{H}} = 8.22$ (s, 1H), 7.60–7.57 (d, $J = 7.5$, 1H), 7.36–7.34 (d, $J = 7.5$, 2H), 7.25–7.13 (m, 3H), 7.01 (s, 1H), 6.74–6.63 (m, 2H), 5.72 (s, 1H), 2.47–2.43 (s, 3H) ppm.

2.8.8 2-(3,4-Dimethoxyphenyl)-2,3-Dihydroquinazolin-4(1H)-One (Entry 5, Table 3)

^1H NMR (400 MHz, DMSO- d_6): $\delta_{\text{H}} = 8.22$ (s, 1H), 7.63–7.61 (d, $J = 7.6$, 1H), 7.27–7.23 (t, $J = 0.8$, 1H), 7.14 (d, $J = 1.6$, 1H), 7.02–6.98 (m, 2H), 6.96 (s, 1H), 6.77–6.75 (d, $J = 8$, 1H), 6.71–6.66 (t, $J = 1.2$, 1H), 5.72 (s, 1H), 3.78 (s, 3H), 3.75 (s, 3H) ppm.

2.8.9 2-(4-Bromophenyl)-2,3-Dihydroquinazolin-4(1H)-One (Entry 9, Table 3)

^1H NMR (400 MHz, DMSO- d_6): $\delta_{\text{H}} = 8.18$ –8.12 (m, 1H), 7.81–7.79 (m, 1H), 7.62–7.58 (m, 3H), 7.46–7.43 (m, 2H), 7.31–7.25 (m, 1H), 6.76–6.71 (d, $J = 19.2$, 1H), 6.72–6.67 (m, 1H), 5.75 (s, 1H) ppm.

3 Result and Discussion

In continuation of our studies on application of new catalysts in organic transformations [14, 15, 26, 27], we decided to prepare a novel heterogeneous catalyst. In this manner immobilized Pd(0)-SMT complex on MCM-41 was synthesized and applied as catalyst for the synthesis of 2, 3-dihydroquinazolin-4(1H)-ones derivatives through the reaction of aromatic aldehydes and anthranilamide and anilines from amination of aryl halides.

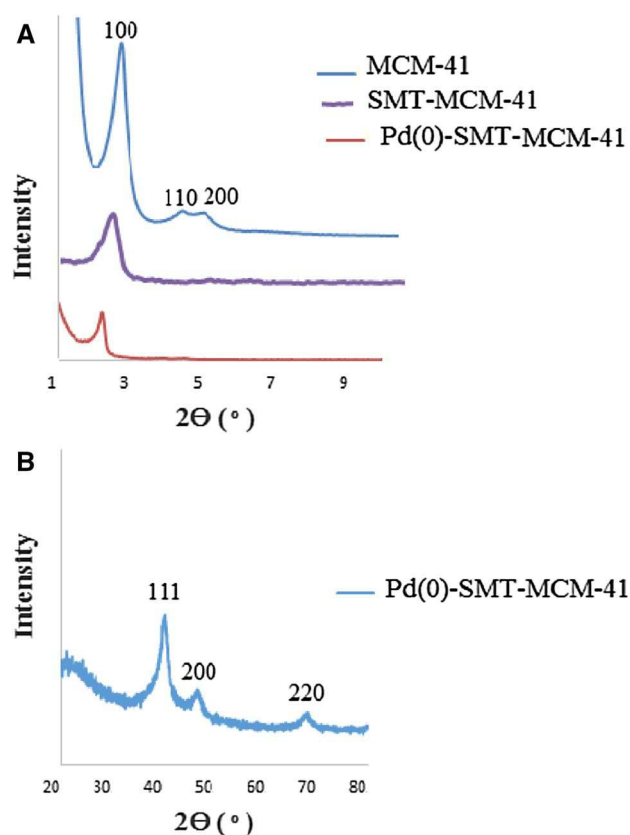


Fig. 1 The XRD patterns of **a** top to down MCM-41, SMT-MCM-41 and Pd-SMT-MCM-41 at low angle **(b)** Pd(0)-MCM-41 at wide angle

The low angle XRD patterns for the MCM-41 and Pd(0)-SMT-MCM-41 catalyst derived by post-synthetic grafting are shown in Fig. 1. The X-ray pattern of the Si-MCM-41 (Fig. 1a) shows a typical three-peak pattern with a very strong reflection at $2\theta = 2.41^\circ$ due to the d_{100} plane and also two other weaker reflections at $2\theta = 3.87^\circ$ and $2\theta = 4.33^\circ$ due to higher order d_{110} and d_{200} planes respectively indicated the formation of a well-ordered mesoporous material with hexagonal symmetry. The functionalized MCM-41 (SMT-MCM-41) presents well-defined (100) reflection in its XRD pattern, however there are no well resolved peaks (110, 200) which are clearly visible corresponding MCM-41 analogs, intensity of the peak at d_{100} was decreased with an increase in loading amount of SMT-MCM-41, which means that the hexagonal mesostructures are less ordered due to successful introduction of SMT-MCM-41 into mesoporous channels of MCM-41. An overall decrease in the intensity of d_{100} was seen, this decrease in intensity was significant for the Pd(0)-SMT-MCM-41 sample. The intensity reduction may be mainly due to contrast matching between the silicate framework and organic moieties which are located inside the pores of mesoporous MCM-41 and also to the irregular immobilization of palladium on the nano channels of MCM-41. Figure 1b indicates the

wide-angle XRD pattern of sample Pd(0)-SMT-MCM-41 in the region $2\theta = 30^\circ\text{--}80^\circ$. Figure 1B shows the reflections at 39.9° , 46.4° and 68.3° where these peaks correspond to (111), (200) and (220) respectively [21]. The typical diffraction pattern of palladium *fcc* crystalline structure is clearly observed, which is in agreement with reported ones in the literature [28].

Thermo gravimetric (TG) analysis of the samples is given in Fig. 2. A one-step weight loss with approximate amount of 6 wt% was observed for Si-MCM-41 which is due to desorption of water. As seen in Fig. 2, three stages of weight loss were observed for Pd(0)-SMT-MCM-41. About 5%, weight loss was observed in the first stage (below 200°C) due to the loss of physically absorbed water and organic solvents. In the second stage ($350\text{--}550^\circ\text{C}$), weight loss is around 10%, which was assigned to the decomposition of covalently bonded organics. The weight loss in the third stage ($450\text{--}800^\circ\text{C}$) is very slight and is about 2%, which may be attributed to the thermal decomposition of silanol groups. The TG curve of Pd(0)-SMT-MCM-41 shows weight loss about (10 wt %) at $200\text{--}450^\circ\text{C}$, which is attributed to loss of grafted immobilized organic groups on the surface of MCM-41. In addition, to calculate the exact percentage of organic groups immobilized on the MCM-41 surface, elemental analysis was carried out that the result is as: C 6.90%, H 1.39%, N 0.39% and S 1.49%.

In order to observe the morphology of the studied surfaces, the synthesized materials have been characterized by Scanning Electronic Microscopy (SEM), Fig. 3a, b are shown micrograph of MCM-41 and Pd(0)-SMT-MCM-41 which confirms the presence of uniform particles size with spherical shape for catalyst. SEM image Pd(0)-SMT-MCM-41 (Fig. 3b) showed no changes occurred during surface modification and morphology of the solid was saved. Moreover, the existence of metallic Pd in

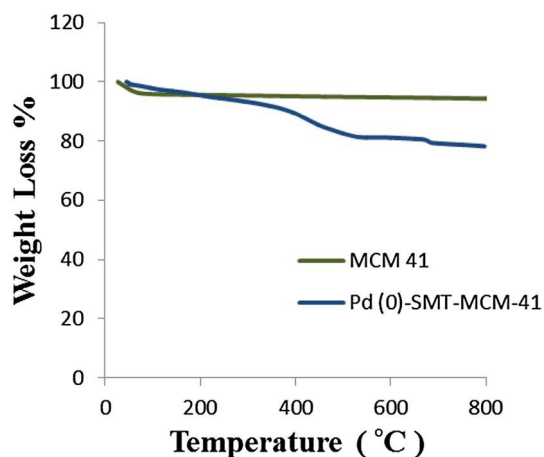


Fig. 2 TGA diagram of (green line) MCM-41 and (blue line) Pd(0)-SMT-MCM-41

Pd(0)-SMT-MCM-41 nanocatalyst was also confirmed by the EDS detector coupled to the SEM which showed the presence of C, Si, N, O, S and Pd in functionalized mesoporous MCM-41 (Fig. 3c). Furthermore, the amount of Pd introduced into the MCM-41 found to be 16.8%, which was obtained by inductively coupled plasma optical emission spectrometry (ICP-OES).

TEM image of the supported Pd(0)-SMT-MCM-41 catalyst is depicted in Fig. 4. It is observed that the well-ordered regular arrangement and also the hexagonal structure were still retained for the supported catalysts. Also, TEM image shows the fine dispersion of palladium particles on the MCM-41. The places with darker contrast could be assigned to the presence of Pd particles. The small dark spots in the image could be attributed to Pd nanoparticles, probably located into the support channels. Furthermore, the larger dark spots over the channels most likely correspond to Pd nanoparticles agglomerates on the external surface.

Figure 5 shows the FT-IR spectra of MCM-41, functionalized-MCM-41, MCM-41-Ligand, catalyst and recovered catalyst. The absorption band around $1080\text{--}1200\text{ cm}^{-1}$ is due to Si-O asymmetric stretching vibrations of Si-O-Si bridges and 460 cm^{-1} corresponding to bending Si-O-Si (Fig. 5a). The spectra of functionalized MCM-41 (Fig. 5b) show C-H stretching vibration at 2932 cm^{-1} . This spectrum also shows that the band attributed to the C-Cl became overlapped by the intense band of the Si-O group at 812 cm^{-1} . In the FT-IR spectrum of MCM-41-ligand (Fig. 5c), the stretching vibration bands at 1300 cm^{-1} (C-N), 1480 cm^{-1} (N-H) and 1655 cm^{-1} (C=N) confirm the presence of *s*-methyl isothiourea onto the pores of mesoporous MCM-41. The free ligand indicated a stretching vibration at 1655 cm^{-1} while in the catalyst this band is shifts to lower frequency and appears at 1642 cm^{-1} indicating the formation of Pd-ligand bond (Fig. 5d). Interestingly, the spectra of the recovered catalyst (Fig. 5e) confirms that the catalyst is stable during the reactions.

Figure 6 shows the N_2 adsorption-desorption isotherms of MCM-41, SMT-MCM-41 and Pd(0)-SMT-MCM-41. Based on the IUPAC classification these samples display a typical type IV adsorption isotherm, indicated the presence of the mesoporous materials. The results for N_2 adsorption-desorption containing the BET surface area (S_{BET}), the total pore volumes (V_{total}), the pore diameters (D_{BJH}) and wall thickness of the calcined MCM-41, SMT-MCM-41 and Pd(0)-SMT-MCM-41 sample are summarized in Table 1. As shown in Table 1, BET analysis of MCM-41 shows a surface area of $986.16\text{ m}^2/\text{g}$ and with upon post synthetic grafting of SMT and then Pd, the catalyst displays a considerably lower BET surface area ($350.25\text{ m}^2\text{ g}^{-1}$) in comparison to the MCM-41. In addition, the pore wall thickness values were

Fig. 3 SEM images of **a** MCM-41, **b** Pd(0)-SMT-MCM-41 and **c** EDS pattern of Pd(0)-SMT-MCM-41

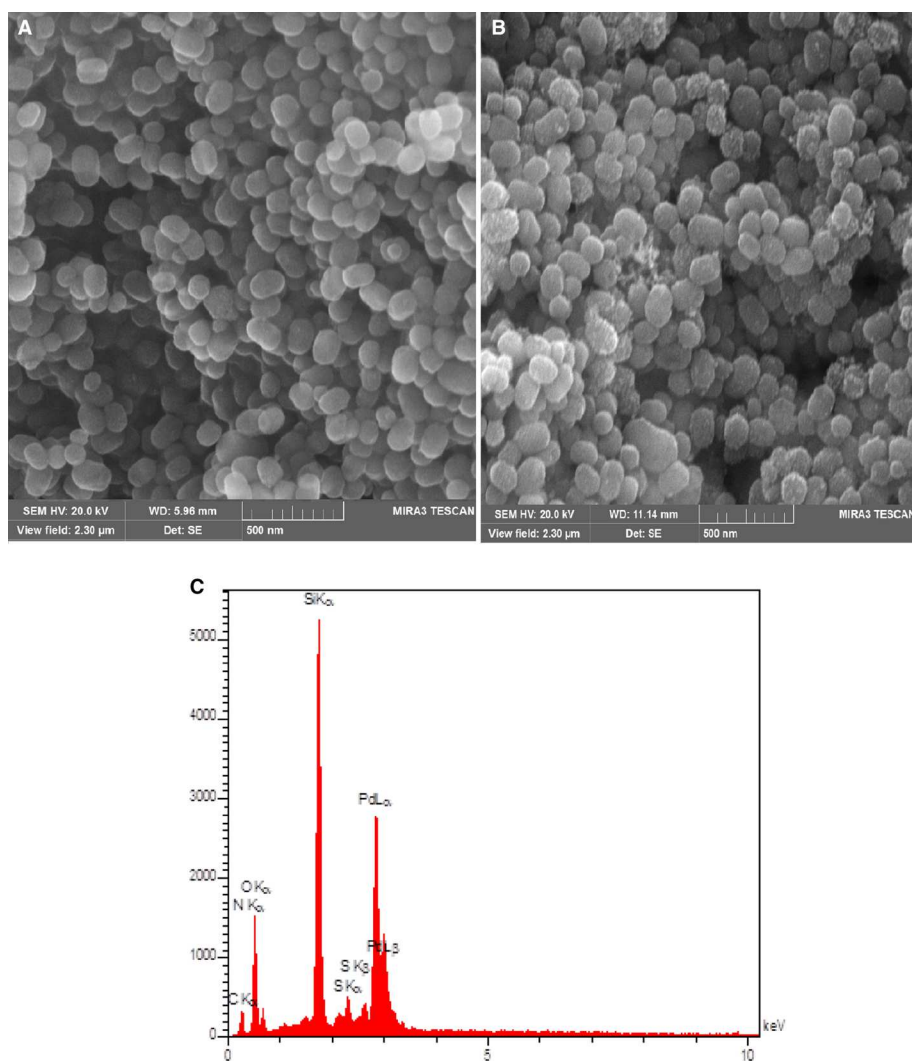
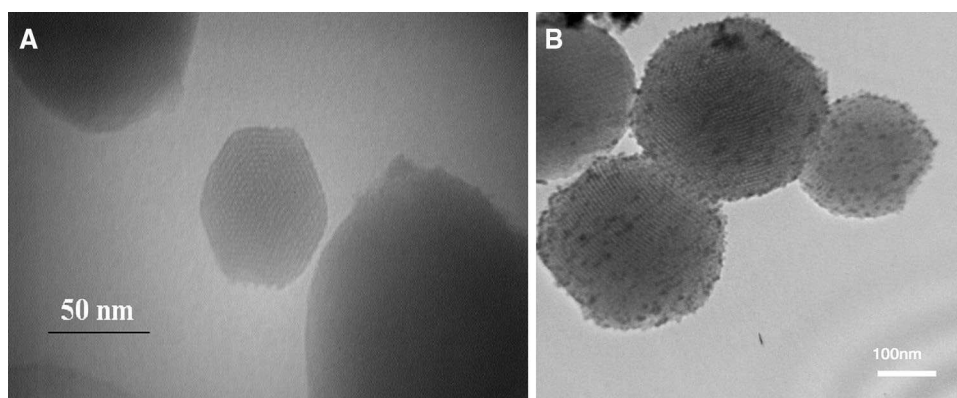


Fig. 4 Transmission electron microscopy (TEM) of MCM-41 (*left*) and Pd(0)-SMT-MCM-41 catalyst (*right*)



calculated to be 0.902, 0.980 and 1.21 nm for MCM-41, SMT-MCM-41 and Pd(0)-SMT-MCM-41 respectively, the nitrogen adsorption–desorption isotherms studies demonstrated that a significant decrease in BET surface area and pore volume and increase of wall thickness of

SMT-MCM-41 and Pd(0)-SMT-MCM-41 in comparison to the corresponding values for MCM-41 clearly indicate that the Pd complex has been immobilized inside the channels/onto the mesoporous wall of the MCM-41 support [29].

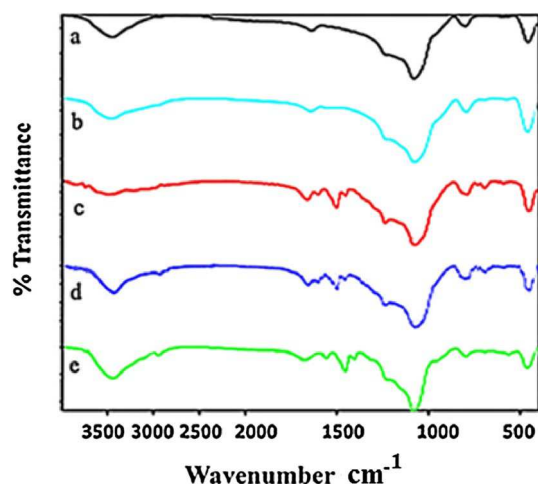


Fig. 5 FTIR spectra of **a** MCM-41, **b** functionalized-MCM-41, **c** MCM-41-ligand, **d** catalyst and **e** recovered catalyst

The results mentioned above confirm that the Pd(0)-SMT-MCM-41 catalyst was synthesized, so the catalytic activity of this synthesized catalyst was investigated in the amination of various aryl halides using aqueous ammonia to produce aniline derivatives (Scheme 2).

In order to optimize the reaction conditions, we chose the iodobenzene as a sample of a non-activated aryl halide with aqueous ammonia as a model reaction and influence of different parameters such as amount of catalyst, nature of solvents and bases were screened and the results are summarized in Table 2.

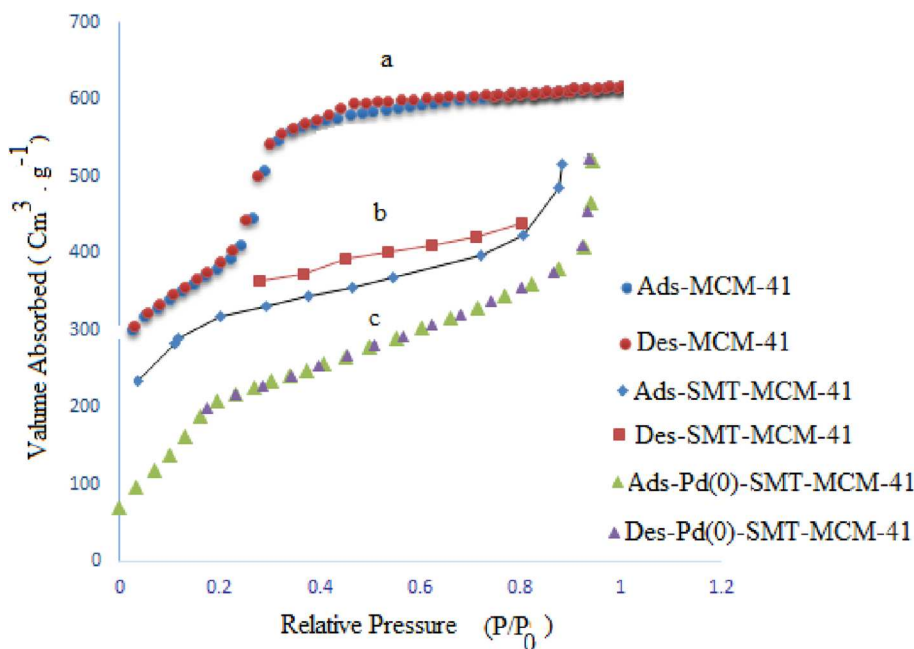
To study the effect amount of catalyst, systematic studies were carried out in the presence of different amounts of the catalyst from 0.1 to 0.2 mol% at room temperature under solvent-free conditions (Table 2, entries 1, 5 and 6). The results show that there is a general trend of increase in isolated yields of products by rising catalyst concentration. Thus, the best yield is found in the presence of 0.2 mol% of Pd (Table 2, entry 1). However, when the higher amount of catalyst (0.2–0.24 mol%) was used, the catalyst still functioned partly well, but the conversion was slight increases in 98% of yield (Table 2, entry 4).

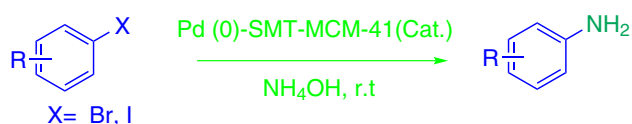
To find the best reaction conditions, the effects of various solvents, such as PEG, DMF, EtOH, DMSO and 1,4-Dioxan were examined (Table 2, entries 7–9). It was found that the reaction didn't complete after 24 h under solvent conditions. Finally, we decided to carry out the amination of aryl halides under solvent-free conditions (Table 2, entry 1).

Table 1 Texture parameters obtained from nitrogen sorption studies

Sample	SBET (m ² /g)	Pore diam by BJH method (nm)	Pore vol (cm ³ /g)	Wall diam (nm)
MCM-41	986.16	3.65	0.711	0.902
SMT-MCM-41	520.10	2.61	0.415	0.980
Pd(0)-SMT-MCM-41	350.25	1.52	0.151	1.21

Fig. 6 Nitrogen adsorption–desorption isotherms of samples **a** MCM-41 **b** SMT-MCM-41 and **c** Pd(0)-SMT-MCM-41 catalyst





Scheme 2 Pd(0)-SMT-MCM-41 catalyzed the amination of aryl halides

Table 2 Optimization of the reaction conditions

Entry	Solvent	Base	Catalyst (mol%)	Time (h)	Yield % ^a
1	—	—	0.2	2.5	96
2	—	—	0.1	2.5	47
3	—	—	0.16	2.5	59
4	—	—	0.24	2.5	98
5	—	—	0.16	5	88
6	—	—	0.1	7	84
7	PEG	—	0.2	24	70
8	DMF	—	0.2	24	65
9	EtOH	—	0.2	24	74
10	DMSO	—	0.2	24	55
11	1,4-Dioxan	—	0.2	80	50
12	—	(Et) ₃ N	0.2	14	90
13	—	Na ₂ CO ₃	0.2	10	85
14	—	K ₂ CO ₃	0.2	8	88
15	—	KOH	0.2	20	75

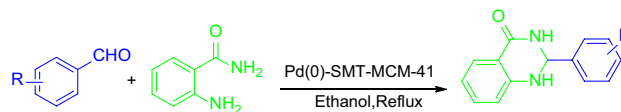
Reaction conditions: iodobenzene (1 mmol), aqueous ammonia (1 mL) at room temperature

^aIsolated yield

In order to find appropriate base we explored the effects of bases on the model reaction under solvent free conditions. The different inorganic and organic bases including (Et)₃N, Na₂CO₃, K₂CO₃ and KOH were examined (Table 2, entries 12–15). As shown in Table 2, it was found that the reaction was performed in absence of base in terms of short reaction time and high yield (Table 2, entry 1).

Subsequently, using the optimized reaction conditions, amination reactions of various electron-poor and electron-rich aryl iodides or bromides derivatives with aqueous ammonia were investigated. The representative results are summarized in Table 3. It was observed that the catalyst exhibits high catalytic activities for coupling of various aryl halides with aqueous ammonia providing excellent yields of desired products.

On the other hand, in order to extend of applications of synthesized catalyst, we explored catalytic activity of [Pd(0)-SMT-MCM-41] as a new heterogeneous and reusable catalyst in the one-pot synthesis of 2,3-dihydroquinazolin-4(1H)-ones through the reaction of aromatic aldehydes and anthranilamide (Scheme 3). In order to determine the most appropriate reaction conditions, the reaction of



Scheme 3 Pd(0)-SMT-MCM-41 catalyzed the synthesis of 2,3-dihydroquinazolin-4(1H)-one derivatives

Table 3 Amination of aryl halides in the presence of Pd(0)-SMT-MCM-41 using aqueous ammonia

1a-1j		2a-2j	

Entry	Aryl halide	Product	Time (h)	Yield (%) ^a	M. p (°C) (References)	TOF(h ⁻¹)
1	Iodobenzene	2a	2.5	96	Oil [10]	192
2	Bromobenzene	2b	3	93	Oil [10]	155
3	4-Bromochlorobenzene	2c	6	91	68–70 [30]	75.83
4	4-Iodotoluene	2d	4	94	43–44 [10]	117.5
5	4-Iodoanisole	2e	5	95	57–58 [30]	95
6	2-bromonaphtalene	2f	14	92	47–49 [10]	32.85
7	4-Bromonitrobenzene	2g	2	97	146–148 [30]	242.5
8	2-bromopyridine	2h	5	95	56–58	95
9	4-Bromophenol	2i	10	96	186–190	48
10	4-Bromobenzonitrile	2j	2.25	94	87–88 [10]	208.88
11	Iodobenzene	–	2.5	No reaction ^b		

Reaction conditions: aryl halide (1 mmol), aqueous ammonia (1 mL) and catalyst (0.2 mol%) at room temperature

^aIsolated yield

^bReaction conditions: the SMT-MCM-41 catalyst was used

Table 4 Optimization for the synthesis of 2,3-dihydroquinazolin-4(1H)-one conditions for the cyclocondensation of 4-chlorobenzaldehyde and anthranilamide as a model substrates under reflux conditions (except for these entries 8–10) for 20 min

Entry	Solvent	Catalyst (mol %)	Temperature (°C)	Yield (%) ^a
1	Ethanol	–	80	Trace ^b
2	Ethanol	0.1	80	35
3	Ethanol	0.16	80	97
3	Ethanol	0.2	80	98
4	Acetonitrile	0.16	80	60
5	Ethyl acetate	0.16	80	77
5	Dichloromethane	0.16	80	45
6	Acetone	0.16	80	63
7	n-Hexane	0.16	80	40
8	Ethanol	0.16	25	35
9	Ethanol	0.16	40	55
10	Ethanol	0.16	60	70

^aIsolated yield

^bAfter 12 h

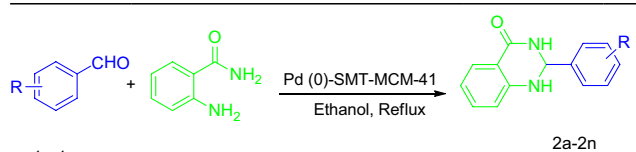
anthranilamide and 4-chlorobenzaldehyde were selected as model substrates and the influence of the amount of catalyst, nature of the solvents and the effect of temperature on the reaction times and yields was studied.

To prove the true effectiveness of the catalyst, the reaction was performed without catalyst. It was found that in the absence of Pd(0)-SMT-MCM-41, the synthesis of 2,3-dihydroquinazolin-4(1H)-ones, did not proceed even after 12 h (Table 4, entry 1). As indicated in Table 4 the best result has been obtained with 0.16 mol % of catalyst in terms of reaction time and isolated yield (Table 4, entry 3). In the next step, the effect of various solvents such as acetonitrile, acetone, ethyl acetate, n-hexane and dichloromethane was investigated by carrying out the model reaction in the presence of Pd (0)-SMT-MCM-41 (Table 4, entries 4–7). As shown in Table 4, among the screened solvents, ethanol is found to be optimal solvent for the synthesis of 2,3-dihydroquinazolin-4(1H)-ones (Table 4, entry 3).

Also, we found that model reaction yields were susceptible to temperature changes. Therefore this reaction was checked under different temperatures including room temperature (25 °C), 40, 60, and 80 °C (Table 4, entries 3 and 8–10). It was observed that the yield increased as the reaction temperature was raised. Thus, temperature 80 °C was the optimal one in this study (Table 4, entry 3).

Using the optimized reaction conditions, this process was demonstrated by the wide range of substituted divers aldehydes electron-donating (Table 5, entries 2–5) and electron-withdrawing (Table 5, entries 6–11) functional groups to synthesize the corresponding products in excellent yields

Table 5 Synthesis of 2,3-dihydroquinazolin-4(1H)-ones catalyzed by Pd(0)-SMT-MCM-41 in ethanol and at 80 °C

						
Entry	Aldehyde	Product	Time (min)	Yield (%) ^a	M. p (°C) (References)	TOF (h ⁻¹)
1	Benzaldehyde	2a	50	96	219–221 [31]	722.8
2	4-Methylbenzaldehyde	2b	25	98	223–226 [23]	1493
3	4-Methoxybenzaldehyde	2c	40	98	178–179 [31]	928
4	4-Ethoxybenzaldehyde	2d	35	97	164–165 [31]	1039
5	3,4-Dimethoxybenzaldehyde	2e	55	96	214–215 [23]	654.5
6	4-Chlorobenzaldehyde	2f	20	97	199–200 [25]	1818.7
7	3-Bromobenzaldehyde	2g	75	98	175–176 [23]	490
8	3-Nitrobenzaldehyde	2h	145	94	215–216 [31]	243.1
9	4-Bromobenzaldehyde	2i	110	95	197–199 [23]	323.8
10	2-Nitrobenzaldehyde	2j	180	93	180–183 [22]	193.75
11	4-Fluorobenzaldehyde	2k	100	97	196–197 [31]	363.75
12	Terephthalaldehyde	2l	25	98	245–246 [31]	1470
13	Cinnamaldehyde	2m	60	92	201–203 [23]	575
14	4-Chlorobenzaldehyde	–	20	No reaction ^b		

Reaction conditions: aldehyde (1 mmol), 2-aminobenzamide (1 mmol), catalyst (0.16 mol%) and solvent (10 mL) at reflux temperature

^aIsolated yield

^bReaction conditions: the SMT-MCM-41 catalyst was used

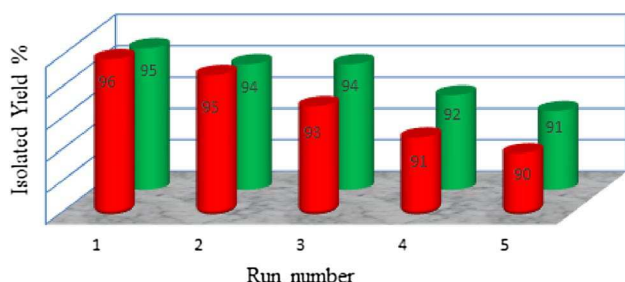


Fig. 7 The recycling experiment of Pd(0)-SMT-MCM-41 in the amination of iodobenzene (green column) and synthesis of 2-(4-chlorophenyl)-2,3-dihydroquinazolin-4(1H)-one (red column)

(Table 5). It is also notable that the electronic property of the aromatic ring of aldehydes has some effects on the rate of the condensation process. Also, terephthalaldehyde (Table 5, entry 12) was successfully employed to prepare the corresponding product in excellent yield

The reusability of the catalysts is an important advantage and makes them useful for commercial applications. The reusability of the Pd(0)-SMT-MCM-41 was investigated for the amination of iodobenzene and synthesis of 2-(4-chlorophenyl)-2,3-dihydroquinazolin-4(1H)-one under the optimized reaction conditions. As shown in Fig. 7, the separated catalyst was reused over five consecutive runs without any significant loss of activity for these reactions.

4 Hot Filtration Test

In order to find out whether the catalyst is truly heterogeneous in nature or whether Pd is leaching out from the solid catalyst to the solution. The heterogeneity of the Pd(0)-SMT-MCM-41 catalyst was examined by carrying out a hot filtration test using anthranilamide and 4-chlorobenzaldehyde as model substrates. In this experiment, after continuing the reaction under optimized conditions, we found the yield of product in half time of the reaction that it was 55%. Then the reaction was repeated and in half time of the reaction, the catalyst was separated from reaction mixture and allowed the filtrate to react further under identical reaction conditions. The yield of reaction in this stage was 58% that confirmed the leaching of palladium hasn't been occurred.

5 Conclusion

In conclusion, Pd(0)-SMT-MCM-41 was synthesized as a new heterogeneous and reusable catalyst. The catalytic activity of Pd(0)-SMT-MCM-41 was probed for amination of aryl halides by aqueous ammonia and the synthesis of a wide range of 2,3-dihydroquinazolin-4(1H)-ones. This system has many advantages, such as the simple methodology,

easy work up, high yields, eco-friendly, simplicity in: separation of catalysts. The results indicate that the activity of the catalyst was not much affected on recycling. Therefore, the catalyst can be reused for five times without any significant loss of activity.

Acknowledgement This work was supported by the research facilities of Ilam University, Ilam, Iran.

References

1. Beck JS, Vartuli JC, Roth WJ, Leonowicz ME, Kresge CT, Schmitt KD, Chu CTW, Olson DH, Sheppard EW, McCullen SB, Higgins JB, Schlenker JL (1992) *J Am Chem Soc* 114:10834–10843
2. Kresge CT, Leonowicz ME, Roth WJ, Vartuli JC, Beck JS (1992) *Nature* 359:710–712
3. Thomas JM, Raja R (2004) *J Organomet Chem* 689:4110–4124
4. Lee YC, Dutta S, Wu KCW (2014) *Chem Sus Chem* 7:3241–3246
5. Li Y, Ma Q, Liu Z, Wang X, Su X (2014) *Anal Chim Acta* 840:68–74
6. Kosslick H, Mönnich I, Paetzold E, Fuhrmann H, Fricke R, Müller D, Oehme G (2001) *Micropor Mesopor Mat* 44:537–545
7. Shu Y, Shao Y, Wei X, Wang X, Sun Q, Zhang Q, Li L (2015) *Micropor Mesopor Mat* 214:88–94
8. Lv L, Wang K, Zhao XS (2007) *J Colloid Interface Sci* 305:218–225
9. Delle Piane M, Corno M, Pedone A, Dovesi R, Ugliengo P (2014) *J Phys Chem C* 118:26737–26749
10. Havasi F, Ghorbani-Choghamarani A, Nikpour F (2015) *New J Chem* 39:6504–6512
11. Polshettiwar V, Len C, Fihri A (2009) *Coord Chem Rev* 253:2599–2626
12. Nadri Sh, Joshaghani M, Rafiee E (2009) *Organometallics* 28:6281–6287
13. Nadri Sh, Azadi E, Ataei A, Joshaghani M, Rafiee E (2011) *J Organomet Chem* 696:2966–2970
14. Nikoorazm M, Ghorbani-Choghamarani A, Mahdavi H, Esmaeili SM (2015) *Micropor Mesopor Mat* 211:174–181
15. Nikoorazm M, Ghorbani-Choghamarani A, Noori N (2015) *Appl Organomet Chem* 29:328–333
16. Hassan HMA, Saad EM, Soltan MS, Betiha MA, Butler IS, Mostafa SI (2014) *Appl Catal A Gen* 488:148–159
17. Hao WY, Ding GD, Cai MZ (2014) *Catal Commun* 51:53–57
18. Yuzawa H, Yoshida H (2010) *Chem Commun* 46:8854–8856
19. Yang BO, Liao L, Zeng Y, Zhu X, Wan Y (2014) *Catal Commun* 45:100–103
20. Yang X, Guan Q, Li W (2011) *J Environ Manag* 92:2939–2943
21. Chen J, Yuan T, Hao W, Cai M (2011) *Tetrahedron Lett* 52:3710–3713
22. Hajjami M, Tahmasbi B (2015) *RSC Adv* 5:59194–59203
23. Ghorbani-Choghamarani A, Norouzi M (2014) *J Mol Catal A Chem* 395:172–179
24. Chena BH, Lia JT, Chen GF (2015) *Ultrason Sonochem* 23:59–65
25. Ghorbani-Choghamarani A, Azadi G (2015) *RSC Adv* 5:9752–9758
26. Nikoorazm M, Ghorbani-Choghamarani A, Noori N (2015) *J Porous Mat* 22:877–885
27. Noori N, Nikoorazm M, Ghorbani-Choghamarani A (2015) *J Porous Mat* 22:1607–1615

28. Song K, Liu P, Wang J, Pang L, Chen J, Hussain I, Li T (2015) Dalton Trans 44:13906–13913
29. Dhara K, Sarkar K, Srimani D, Kumar Saha S, Chattopadhyay P, Bhaumik A (2010) Dalton Trans 39:6395–6402
30. Thakur KG, Srinivas KS, Chiranjeevi K, Sekar G (2011) Green Chem 13:2326–2329
31. Rostami A, Tahmasbi B, Gholami H, Taymorian H (2013) Chin Chem Lett 24:211–214